



Emission dispersion modeling and geospatial analysis of vehicular emissions in some parts of Benin City, Nigeria

I. R. Ilaboya ^{a,*}, E. A. Oturo ^b

^a Department of Civil Engineering, University of Benin, P.M.B 1154, Benin City, Nigeria

^b Department of Civil Engineering, Nigeria Maritime University, Okerenkoko, Nigeria

ARTICLE INFO

Article history:

Received 26 November 2020

Received in revised form
17 December 2020

Accepted 28 December 2020

Available online
29 December 2020

Keywords:

Air pollution

Cross validation

Geospatial analysis

Prediction maps

Vehicular emission

ABSTRACT

Over the years, decline in air quality has been connected to the growing rate of urbanization and increasing number of vehicles on the roads. Most of the pollutants emitted from vehicular activities have been observed to have adverse effects on individuals as well as the atmosphere. Although, the focus of this study is to develop an emission dispersion model to predict the concentration of specific air pollutants with distance, the application of geostatistical technique such as Kriging interpolation to study the spatial distribution of pollutants from vehicular emissions around the study area was also exemplified. Seven (7) georeferenced points, namely, Ugbowo main gate, Ekosodin junction, Agen junction, Super D junction, Nitel junction, Okhunmwun junction and Oluku market junction were used for data collection. Pollutants from vehicular emissions, namely, nitrogen dioxide (NO₂), carbon monoxide (CO) including the total radiation were monitored in the morning and evening for a period of 35 days (7th July to 12th August 2020) with the aid of portable toxic gas monitors and radiation alert meters. Other parameters of interest, which were also measured include maximum temperature and wind speed using infra-red thermometers and portable anemometer respectively. To ascertain the quality of the data, selected preliminary analysis, namely, test of normality, test of homogeneity, outlier detection and reliability test were done. Result of the study showed a high concentration of NO₂, CO and total radiation around Ugbowo main gate and Okhunmwun community and environs especially during the peak hours of evening (5.0 p.m. – 6.0 p.m.) when the traffic load is high.

1. Introduction

Transportation is one of the main sources of air pollution in many countries due to the increasing numbers of vehicle present on the road at every particular time [1],[2]. The number of vehicles is continuously rising with population growth and purchasing power. In

general, the effects of vehicular emission on the people are most intense in large urban centers apparently due to numerous emission sources, unfavorable dispersion characteristics and high population densities [1]–[4].

Air pollutants emitted from cars are believed to increase the risk of stroke, lung cancer, chronic and acute respiratory diseases

* Corresponding author

E-mail address: rudolph.ilaboya@uniben.edu
<https://doi.org/10.37121/jase.v4i1.143>

such as asthma, heart disease, birth defects and eye irritation [5]. For pregnant women who are exposed to polluted air, there is the likelihood of pregnancy and birth related-issues including preterm births [6]. Emerging evidence has also revealed that ambient air pollution may result to diabetes and neurological development in children. In addition, some air pollutants and particulate matter from cars can be deposited on soil and surface waters [7] that eventually enters the food chain where they get into the human bio-system. These substances can affect the respiratory, reproductive, immune as well as the neurological systems of animals [5].

The dearth of air quality data in Nigeria and most parts of Africa, results in low regional levels of awareness about the resultant effects of air pollution and limits people's capacity to protect their health [8]. Emerging reports have placed the continent of African as the one with the most notable regions with shortage of accessible air quality monitoring data, while facing several challenges related to air quality in the region [9]. It also has one of the highest rates of rural-urban migration compared to any other region with growing numbers of the population moving to urban cities where air pollution levels tend to be on the increased [10]. In Nigeria, vehicular emissions are significantly on the rise due to lack of good transportation systems, giving way for unworthy road vehicles and unchecked use of private vehicles on the roads [11].

2. Methodology

2.1. Description of Study Area

The study area is limited to some parts of Benin City, particularly Ugbowo and environs where serious traffic jam is experienced on daily basis. From the onset and even now, Benin city remains the principal administrative and socio-economic center for both Oredo Local Government Area (LGA) and Edo state in Nigeria. Benin city is a humid tropical urban settlement that comprises three LGAs (Oredo, Egor and Ikpoba-Okha). This city, which is located within latitudes 6°20'N and 6°58'N and longitudes 5°35'E and 5°41'E, broadly occupies an area of approximately 112.552 km². This widespread coverage suggests spatial variability of weather and climatic elements [12]. Benin City lies visibly in the southern most corner of a dissected margin; a prominent topographical unit that lies north of the Niger Delta, west of the lower Niger valley, and south of the Western plain [13]. The

specific locations employed for data collection are presented in Fig. 1.

2.2. Data Collection and Preliminary Analysis

Seven (7) georeferenced points, namely; Ugbowo main gate, Ekosodin junction, Agen junction, Super D junction, Nitel junction, Okhunmwun junction and Oluku market junction were used for data collection. Pollutants from vehicular emission, namely, nitrogen dioxide (NO₂), carbon monoxide (CO) including the total radiation were monitored in the morning (9 a.m. – 10 a.m.) and evening (5 p.m. – 6 p.m.) for a period of 35 days (7th July to 12th August 2020) with the aid of Aeroqual multi-parameter environmental monitor (series 500) and radiation alert meter. Other parameters of interest, which were measured include maximum temperature and wind speed using infra-red thermometers and Sky master thermo anemometer (SM-28) respectively. The duration of measurement, including the calibrated unit of the gas detector is presented in Table 1.

The Global Positioning System (GPS) receiver and point positioning techniques were used to obtain the geographical coordinates at each monitoring location in the study area. The coordinates were converted to decimal degrees format using the Universal Traverse Mercator (UTM) software version 1.0. The maximum concentration of each monitored pollutant during the monitoring period was selected and recorded for data processing. The data obtained in parts per million (ppm) were processed by converting the pollutants concentrations from ppm to mg/m³ or µg/m³, using the model of equation (1) presented by [15]. This is because the pollutants hourly or daily or annually concentrations are measured in mg/m³ or µg/m³ [16].

$$\text{Concentration}(\text{mg}/\text{m}^3) = \left(\frac{\text{Conc.}(\text{ppm}) \times \text{GMW}(\text{g}/\text{mole})}{22.4} \right) \quad (1)$$

Where; mg/m³ is the milligram per cubic meter, equal to 10⁻³g/m³; GMW is the gram molecular weight of the pollutant, and the 22.4 is the molar volume of gas at standard temperature and pressure.

To ascertain the quality of the data, selected preliminary analysis using different statistical techniques, namely, test of homogeneity of data using the residual mass curve as proposed by [17], autocorrelation test used to determine the error propagation, outlier detection using seasonal box plot method as proposed by [18], test of normality using

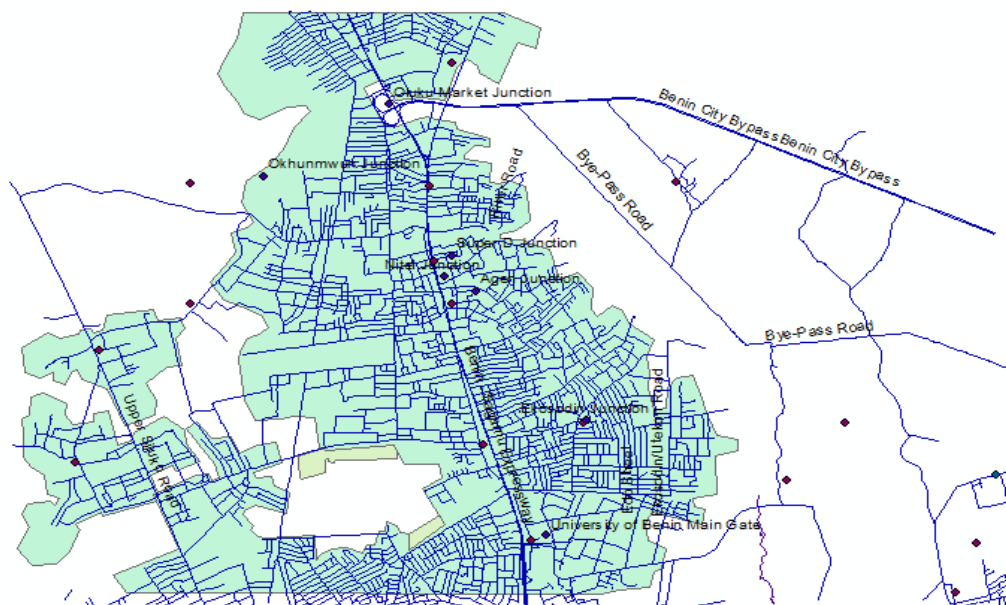


Fig. 1 Map of study area [14].

Table 1 Measurement procedures and equipment used.

Pollutants	Daily duration of Exposure		Equipment	Unit
	Period	Duration (h)		
Temperature	Morning session	1	infra-red thermometers	°C
	Evening session	1		
NO ₂	Morning session	1	Aeroqual multi-parameter environmental monitor (series 500)	ppm
	Evening session	1		
CO	Morning session	1	Aeroqual multi-parameter environmental monitor (series 500)	ppm
	Evening session	1		
Total Radiation	Morning session	1	Radioactive alert meter	µg/m ³
	Evening session	1		

Jarque-Bera method and test of reliability using one-way analysis of variance were done.

2.3. Modeling Ground Level Concentration of Pollutants

Using the concept of Gaussian dispersion model, empirical equation for determining the ground level concentration of gaseous pollutants was developed for the study area. To ascertain the influence of the pollutants on existing atmospheric conditions, gaseous emission dispersion model was developed using the popular adiabatic lapse rate and Pasquill stability index proposed by [15].

2.4. Geospatial Analysis

For the spatial distribution of the pollutants, geospatial analysis using Kriging interpolation method was employed. The following steps are involved in the use of Kriging interpolation method for the geospatial analysis of selected air pollutants:

- evaluation of normality test;
- selection of attribute data and model interpolation method;

- semi-variogram fitting and testing;
- cross validation;
- spatial dependency determination; and
- creation of air quality prediction maps.

3. Results and Discussion

The descriptive statistics of air quality data employed for the study is presented in Table 2. The result shows a high concentration of carbon monoxide and total radiation at peak hour of the day (5 p.m. to 6 p.m.). At this time, market women, business men/women including street traders and hawkers are in a rush to get home as such the traffic situation at this point are usually very high. It is expected that the concentration may be higher than what is experienced presently when society recovers from the current pandemic occasioned by the corona virus. The underlying statistics of homogeneity was formulated as follows:

H0: Data are statistically homogeneous.

H1: Data are not homogeneous.

The null and alternate hypothesis were tested at 90 %, 95 % and 99 % confidence

interval, that is, 0.1, 0.05 and 0.01 degrees of freedom and the result obtained is presented in Fig. 2.

For a homogeneous record, it is expected that the data points fluctuate around the zero-center line of the residual mass curve [19]. From the result of Fig. 2, it was observed that the NO₂ data fluctuate around the zero-center line of the residual mass curve, an indication that the data are statistically homogeneous.

The same approach was employed to assess the homogeneous nature of CO and total radiation data. To check for the occurrence of trend and error propagation in the data, autocorrelation plots and autocorrelation functions were generated from the correlogram of the air quality data using EViews 9.0. Results of autocorrelation plot of radiation data are presented in Fig. 3.

Table 2 Descriptive statistics of air quality data.

Pollutants	Session	Mean	Std. deviation	N
Temperature	Morning session	30.549	1.3716	245
	Evening session	28.879	1.1788	245
	Total	29.714	1.5268	490
NO ₂	Morning session	0.0181	0.01119	245
	Evening session	0.0230	0.01282	245
	Total	0.0206	0.01226	490
CO	Morning session	0.5428	0.36396	245
	Evening session	0.6169	0.32395	245
	Total	0.5799	0.34618	490
Total Radiation	Morning session	0.247	0.1285	245
	Evening session	0.281	0.1298	245
	Total	0.264	0.1302	490

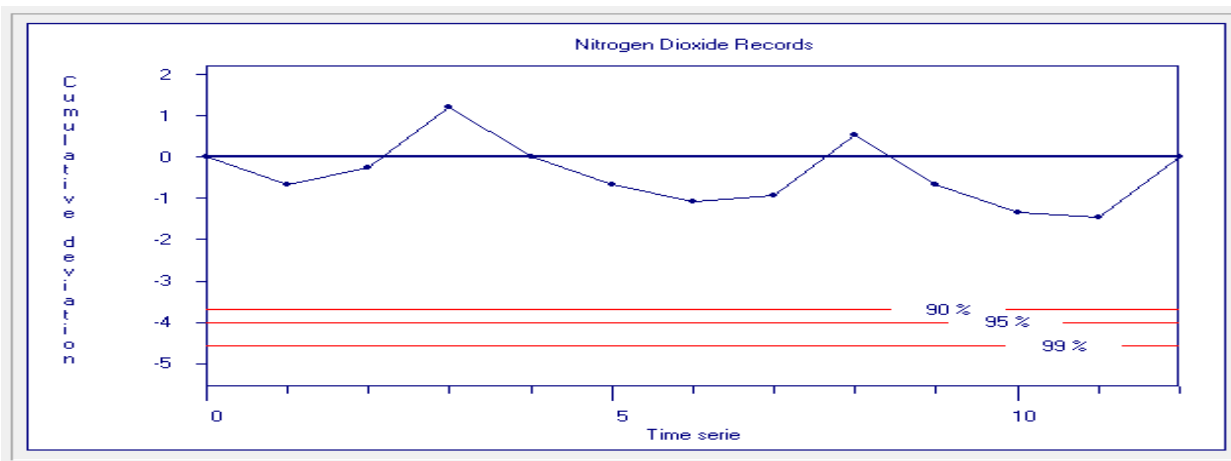
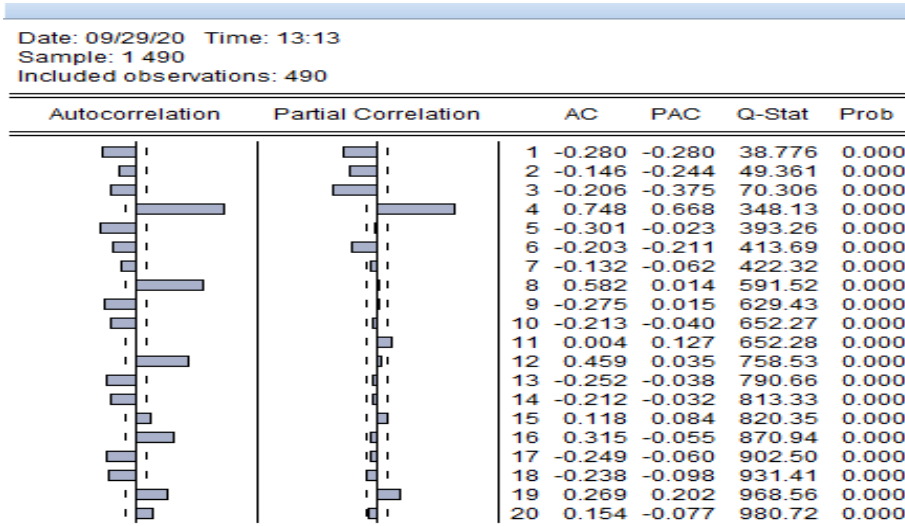


Fig. 2 Homogeneity test of NO₂ data.



AC: autocorrelation; PAC: partial autocorrelation

Fig. 3 Autocorrelation test of NO₂ data.

If the values of the computed auto-correlation function (AC) decrease or fluctuate steadily from top to bottom and tend towards zero, then, it can be concluded that trend exists in the data. Otherwise, it is declared that no observable trend exists in the data. From the result of Fig. 3, it was observed that the calculated autocorrelation functions for NO₂ data fluctuate steadily from top to bottom. Hence, it is concluded that there exist the presence of trend and variability in the air quality records. To ascertain the normality of the data, Jarque-Bera test statistics was computed and presented in Fig. 4.

The calculated Jarque-Bera test value was observed to be 20.50813. Since the Jarque-Bera test value is greater than 10 with a (p-value) that is less than the 5 % significant value, the null hypothesis of normality was rejected. Hence, it is concluded that the measured NO₂ records did not follow a normal distribution [20]. This is expected owing to the influence of temperature and wind speed on the dispersion of gaseous air pollutants. The same approach was applied to other pollutants

and the results showed a non-normally distributed trend. On whether the data employed for the analysis is devoid of outlier, the seasonal box plot presented in Fig. 5 was employed.

The presence of outlier is normally indicated with a square box or circle containing a number inside it [21]. This is not noticeable in Fig. 5. Hence, it is concluded that the measured NO₂ data were devoid of possible outlier. The same approach was applied to other pollutants and the results showed that all the variables (air quality data) are devoid of outlier.

To ascertain the reliability of the data, two-way mixed model having a confidence interval of 95 % (p-value = 0.05) and initial test value of zero (0) was employed. The null hypothesis of reliability was formulated as follows:

H0: Data are reliable.

H1: Data are not reliable.

Using the Fisher's probability test (F-test), the analysis was conducted and the one-way analysis of variance (ANOVA) table was generated and presented in Table 3.

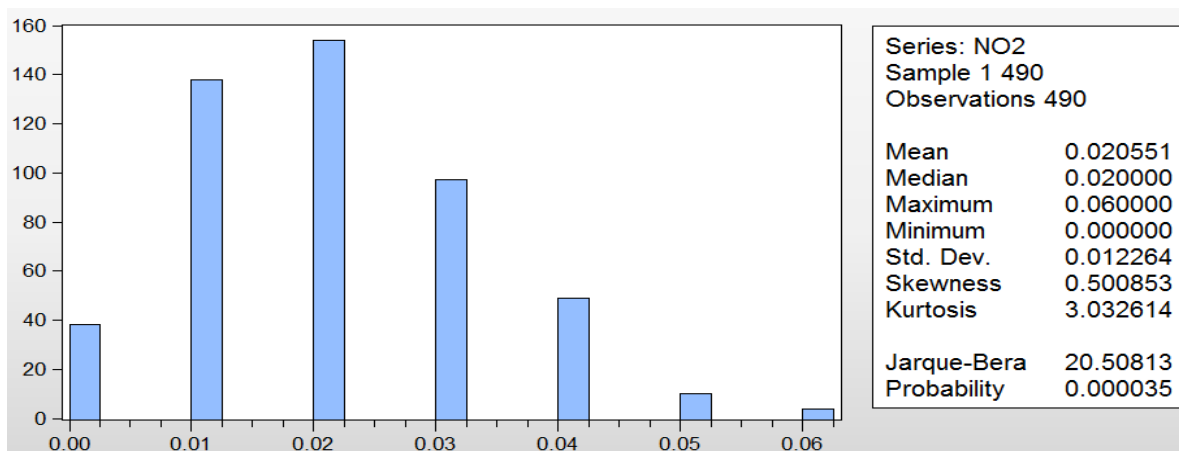


Fig. 4 Normality test result of NO₂ records around the study area.

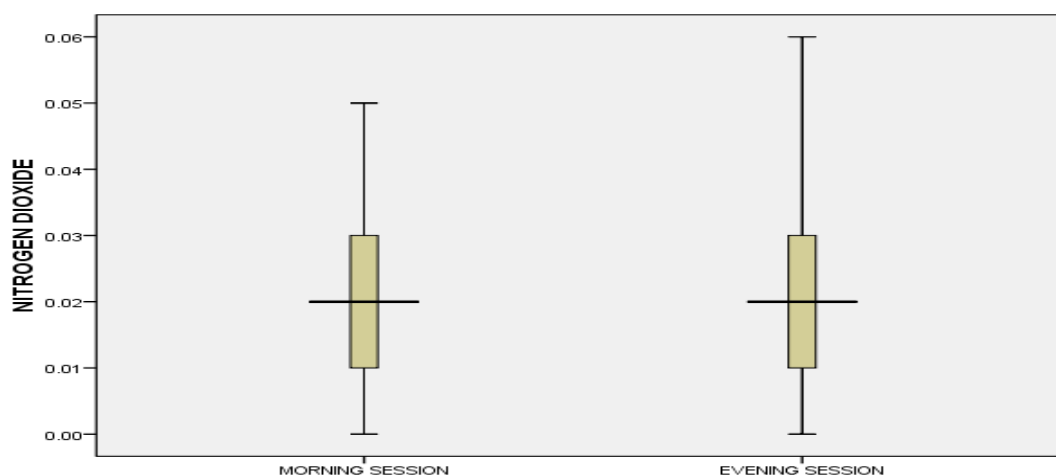


Fig. 5 Seasonal box plot for assessing the presence of outliers in NO₂ data.

Table 3 Analysis of variance table.

		Sum of squares	df	Mean square	F	Sig.
Between people		282.353	489	0.577		
Within people	Between items	318289.685	3	106096.562	1.683E5	0.000
	Residual	924.584	1467	0.630		
	Total	319214.269	1470	217.153		
Total		319496.622	1959	163.092		

Grand Mean = 7.6446

At 0.05 df, with a computed p-value of 0.000 as observed in Table 3, the null hypothesis is accepted and it is concluded that the data are good and can be employed for further analysis. The first step in developing the dispersion model is to determine the nature of the environment based on the elevation and temperature data. From the field measurement for one of the designated stations, the corresponding temperature at station point (elevation of 0 m) was recorded as 31.6 °C while the corresponding temperature at 500 m elevation was observed to be 28.2 °C. Using the equation of adiabatic lapse rate (ALR):

$$ALR = \frac{\partial T}{\partial Z} = \frac{T_2 - T_1}{Z_2 - Z_1} \quad (2)$$

$$ALR = \frac{28.2 - 31.6}{500 - 0} = -0.68 \text{ }^\circ\text{C}/100\text{m.} \quad (3)$$

Where, ∂T is the difference in temperature and ∂Z is the difference in elevation.

The nature of the environment was determined from the ALR diagram (Fig. 6). Based on the diagram, it was observed that the nature of environment around the designated station was highly unstable. From the field data, the maximum wind speed around the station was observed to be 2.33

m/s while the incoming solar radiation was observed to be slightly strong throughout the monitoring period. Based on this information and using the Pasquill stability index presented in Table 4, the stability class for the designated station was determined to be stability class B. Knowing the nature of the environment and the stability class, Table 5 was then employed to determine the vertical and horizontal dispersion coefficient of the gaseous emission around the designated station.

To develop the dispersion model for ground level concentration, Gaussian plume dispersion equation for point source pollution at ground level was adopted as follows:

$$C_{(x,y,z)} = \frac{Q}{\pi U \delta_y \delta_z} \quad (4)$$

Where, Q is the emission rate of pollutant ($\mu\text{g/s}$), U is the average wind speed (m/s), δ_y and δ_z is the horizontal and vertical dispersion coefficient (m), respectively, and Π is a constant term (= 3.142).

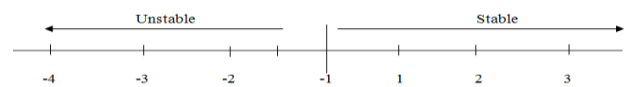


Fig. 6 Adiabatic lapse rate diagram.

Table 4 Pasquill stability types [15].

Surface wind speed (m/s)	Day			Night	
	Incoming solar radiation			Mostly overcast	Mostly clear
	Strong	Moderate	Slight		
>2	A	A-B	B		
2	A-B	B	C	E	F
4	B	B-C	C	D	E
6	C	C-D	D	D	D
>6	C	D	D	D	D

A - Extremely unstable; B - Moderately unstable; C - Slightly unstable; D - Neutral; E - Slightly stable; F - Moderately stable.

Table 5 Dispersion coefficient (m) for selected distance downwind (km) [22].

Distance (km)	Stability class and δ_y						Stability class and δ_z					
	A	B	C	D	E	F	A	B	C	D	E	F
0.2	50	37	25	16	12	8	29	20	14	9	6	4
0.4	94	69	46	30	22	15	84	40	26	15	11	7
0.6	135	99	66	43	32	22	173	63	38	21	15	9
0.8	174	128	85	56	41	28	295	86	50	27	18	12
1	213	156	104	68	50	34	450	110	61	31	22	14
2	396	290	193	126	94	63	1953	234	115	51	34	22
4	736	539	359	235	174	117	-	498	216	78	51	32
8	1367	1001	667	436	324	218	-	1063	406	117	70	42
16	2540	1860	1240	811	602	405	-	2274	763	173	95	55
20	3101	2271	1514	990	735	495	-	2904	934	196	104	59

The basic assumptions made are as follows:

- (a) no cross-wind effect ($y = 0$);
- (b) pollution source at ground level ($H = 0$);
and
- (c) pollutant has reached ground level ($z = 0$).

Hence, pollutant concentration at 8000 m downwind can be calculated as follows;

$$C(8000) = \frac{Q}{3.142 \times 2.33 \times 1001 \times 406} \mu\text{g}/\text{m}^3. \quad (5)$$

Equation (5) is the Gaussian plume model, which can be employed to calculate the downwind concentration of gaseous emission at a distance x along the center line around the designated station provided the emission rate of the pollutant is known. To study the spatial distribution of the measured air pollutants around the study area, four semi-variogram models, namely; stable, circular, spherical and exponential were fitted for geostatistical analysis in order to select the best fitted model. Using the different model, parameters of the semi-variogram were generated. The semi-variogram parameters for NO_2 records are presented in Table 6.

Table 6 Semi-variogram parameters for NO_2 .

Model type	Nugget	Major range	Partial sill
Stable	0.000067	0.1132078	0.000011
Circular	41.563	1.665431	102.566
Spherical	48.094	1.665431	111.986
Exponential	40.452	1.665431	98.674

Table 6 shows the result of semi-variogram parameters for NO_2 and the corresponding values of nugget (the variability in the field data that cannot be explained by distance between the observations), major range (the distance at which two observations are unrelated/independent) and sill (the semi-

variance at which the leveling takes place). The difference between the sill and the nugget is called partial sill. To select the model that best fits the measured data, which can be employed to generate the final prediction map, selected goodness of fit statistics, namely; Root mean square error (RMSE), Mean square error (MSE), Root mean square standardized error (RMSSE) and Average standard error (ASE) generated from the cross-validation step were employed. Estimated goodness of fit statistics corresponding to the different models is presented in Table 7. Based on the estimated RMSE, the best model for each of the four critical parameters was selected and presented in Table 8.

The sill (C) is the summation of nugget and partial sill while the ratio of nugget (C_n) to sill (C) was employed to measure the degree of spatial structure (dependence) [23]. The variable: has a strong spatial dependence, if the ratio is less than 25%; has moderate spatial dependence, if the ratio is between 25% and 75%; and shows only weak spatial dependence, if the ratio is greater than 75% [24]. The computed spatial dependence for the selected gaseous pollutants using the best fit model is presented in Table 9.

Result of Table 9 showed that the gaseous parameters showed relatively strong degree of spatial dependency that made it possible to generate the spatial distribution map for the selected variables. Finally, the prediction map, which can be employed to predict the concentration of vehicular emission around the study area was generated and presented in Figs. 6, 7 and 8 representing NO_2 , CO and total radiation for evening sessions.

Table 7 Calculated cross validation statistics for NO_2 .

Model type	RMSE	MSE	RMSSE	ASE
Stable	0.008852	-0.031944	1.003565	0.008837
Circular	3.095641	-0.099543	1.009953	9.287345
Spherical	4.580972	-0.088564	1.088752	9.266554
Exponential	9.008642	-0.074562	1.014465	9.11982

Table 8 Summary table for estimating spatial dependence.

Parameter	Best model	Nugget	Major range	Partial sill
NO_2	Stable	0.000067	0.1132078	0.000011
CO	Stable	0.00671	0.1132078	0.118421
Total Radiation	Stable	0.00011	0.0560795	0.0042554

Table 9 Estimated spatial dependence of air quality parameters.

Parameter	Best model	Nugget (C_n)	Partial sill	Sill (C)	C_n/C	Degree of spatial dependency
NO_2	Stable	0.000067	0.000011	0.000078	0.859	Strong
CO	Stable	0.00671	0.118421	0.125131	0.054	Strong
Total Radiation	Stable	0.00011	0.0042554	0.0043654	0.0252	Strong

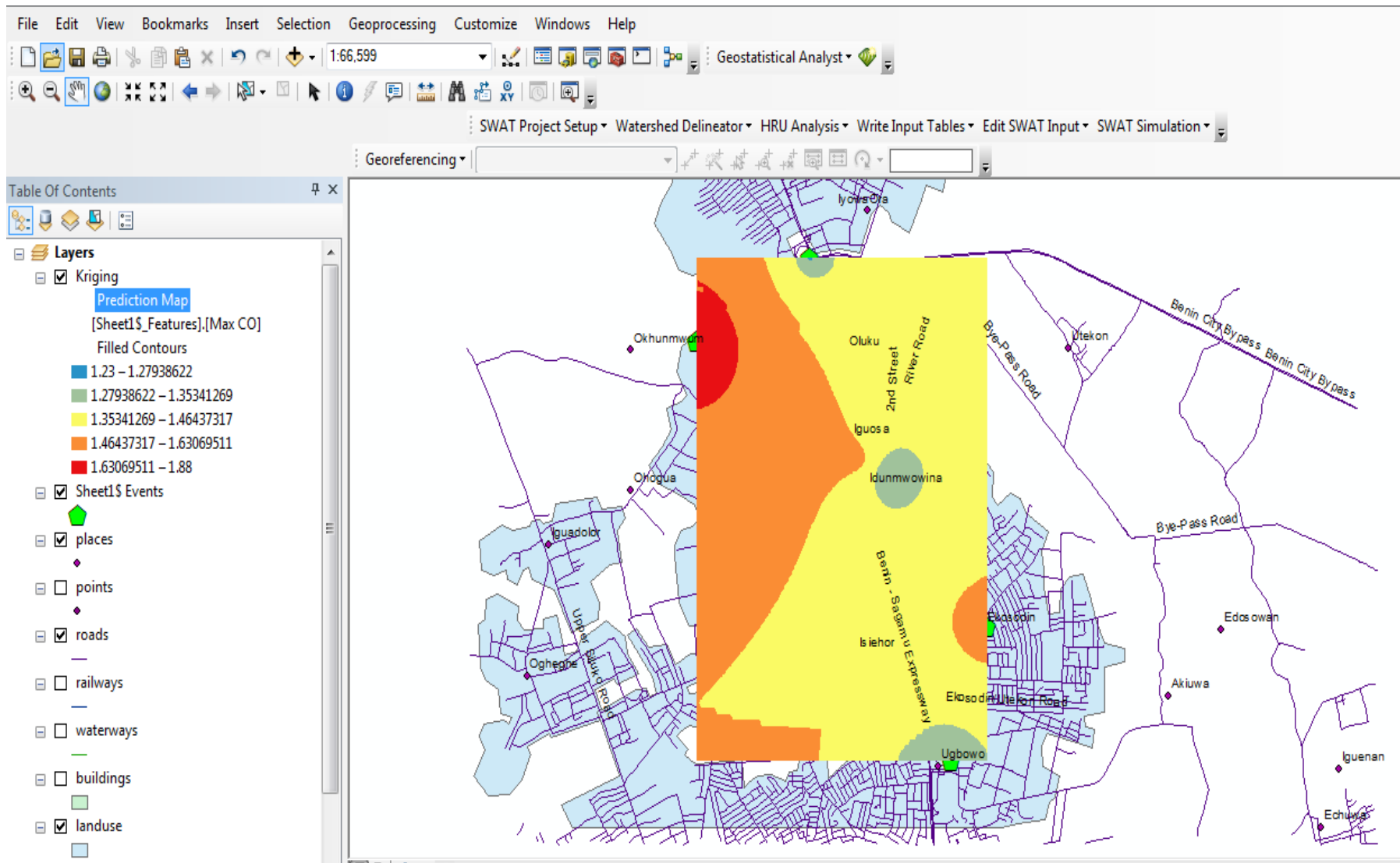


Fig. 7 Final prediction map for the spatial distribution of CO (evening session).

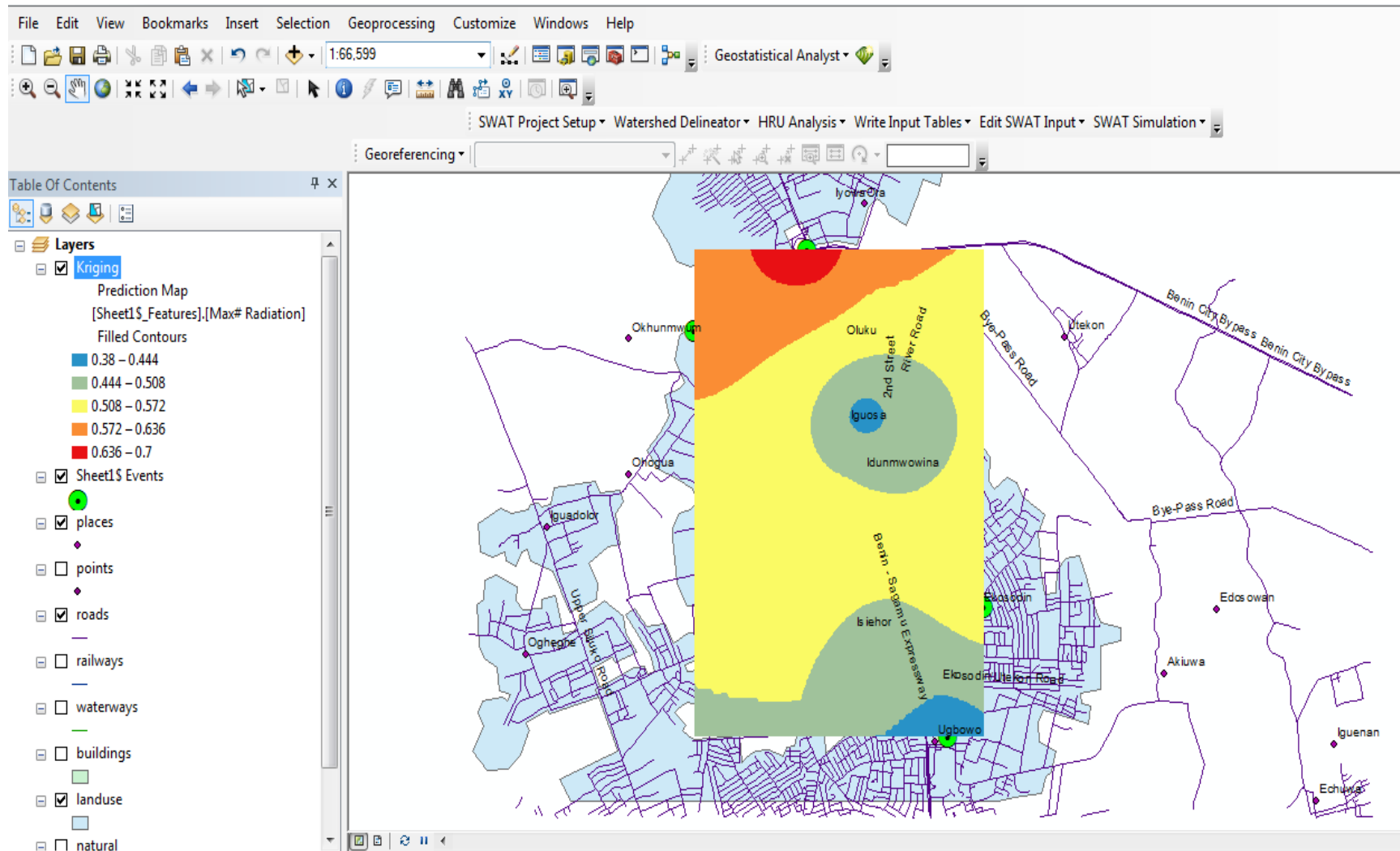


Fig. 8 Final prediction map for the spatial distribution of total radiation (evening session).

Table 10 Ground level results of gaseous pollutants.

Stations	Okunmwun			Ugbowo		
	NO ₂	CO	Total Radiation	NO ₂	CO	Total Radiation
1	0.055	1.650	0.588	0.063	1.334	0.467
2	0.057	1.830	0.597	0.058	1.276	0.394
3	0.054	1.670	0.654	0.062	1.304	0.388
4	0.059	1.890	0.604	0.063	1.331	0.405
5	0.062	1.720	0.527	0.060	1.306	0.412

Areas with red color codes represent higher values of NO₂, CO and total radiation. From the result of Fig. 6, it was observed that high concentration of NO₂ is present around Ugbowo main gate and Okhunmwun community. From the result of Figs. 7 and 8, high concentration of CO and total radiation was observed around Okhunmwun community and environs especially during the peak hours of evening when the traffic load is high. To validate the result of geospatial analysis, five (5) designated points were mapped out around Ugbowo main gate and Okhunmwun community and the concentration of NO₂, CO and total radiation were measured at peak hours (5 p.m. – 6 p.m.) as presented in Table 10.

Table 10 provides the ground-level verification of the spatial distribution maps presented in Figs. 6, 7 and 8. Concentration of gaseous pollutants (NO₂, CO and total radiation) were measured at designated locations in order to validate the results of geospatial analysis and it was observed based on the results of Table 10 that a reasonable agreement exists between the predicted values of the concentration of gaseous pollutants based on geospatial analysis using Kriging interpolation and the observed value obtained using Aeroqual multi-parameter environmental monitor. It suggests therefore, that geospatial analysis is a useful and reliable tool for the prediction of gaseous pollutant concentration.

4. Conclusion

In this study, attempt has been made to develop a dispersion model for predicting vehicular emission concentration around the study area. In addition, a spatial distribution map has also been developed to understand the distribution of vehicular emission around the study area and also estimated the concentration of gaseous pollutants in unsampled locations. From the results of the final prediction map for the spatial distribution of NO₂, CO and total radiation deduced in this study, it was observed that the zone of

influence is Okhunmwun and Ugbowo areas. Although, the span of data used in this paper is not entirely exhaustive of the area under discussion, it has provided additional information on the use of geostatistical technique for the spatial analysis of vehicular emissions, which can form the basis for future studies in related areas.

Conflict of Interests

The authors declare that there is no conflict of interests regarding the publication of this paper.

ORCID

I. R. Ilaboya  <https://orcid.org/0000-0002-8982-7404>

References

- [1] C. Khandar, and S. Kosankar, "A review of vehicular pollution in urban India and its effects on human health," *J. Adv. Lab. Res. Biol.*, vol. 5, no. 3, pp. 54-61, 2014.
- [2] P. Gireesh Kumar, P. Lekhana, M. Tejaswi, S. Chandrakala, "Effects of vehicular emissions on the urban environment- a state of the art," *Mater. Today: Proceedings*, [in press], <https://doi.org/10.1016/j.matpr.2020.10.739>
- [3] A. A. Adeyanju, and K. Manohar, "Effects of vehicular emission on environmental pollution in Lagos," *Sci-Afric J. Sci. Issues. Res. Essays*, vol. 5, no. 4, pp. 34-51, 2017.
- [4] H. S. Huboyo, W. Handayani, and B. P. Samadikun, "Potential air pollutant emission from private vehicles based on vehicle route," IOP conference series: Earth and Environmental Science, vol. 70, no. 1, pp. 1-8, 2017.
- [5] B. Onursal, and S. G. Gautam, "Vehicular air pollution: experiences from seven Latin American urban centers," World Bank technical paper no. 373, Washington, D.C.: The World Bank Latin American and the Caribbean Region Technical Department, 1997.
- [6] R. Afroz, M. N. Hassan, and N. A. Ibrahim, "Review of air pollution and health impacts in Malaysia," *Environ. Res.*, vol. 92, no. 2, pp 71-77, 2003.
- [7] J. King, "How does car pollution affect the environment & ozone layer?" December 27,

2018. [Online]. Available <https://homeguides.sfgate.com/car-pollution-affect-environment-ozone-layer-79358.html> [Accessed Dec. 17, 2020]
- [8] E. U. Etim, "Air pollution emission inventory along a major traffic route within Ibadan metropolis, southwestern Nigeria," *Afr. J. Environ. Sci. Technol.*; vol. 10, no. 11, pp. 432-438, 2016.
- [9] World Air Quality Report, Region & City PM2.5 Ranking, IQAir AirVisual, 2018, Retrieved from <https://www.swissairpurifier.co.za/wp-content/uploads/2019/04/2018-World-air-quality-report-.pdf> [Accessed: Dec. 17, 2020]
- [10] F. I. Abam, and G. O. Unachukwu, "Vehicular emissions and air quality standards in Nigeria," *Eur. J. Sci. Res.*, vol. 34, no. 4, pp. 550-560, 2009.
- [11] U. G. Akpan, and P. N. Ndoke, "Contribution of vehicular traffic emission to CO₂ emission in Kaduna and Abuja," Federal University of Technology, Minna, Nigeria, 1999.
- [12] N. M. Nwokediuko, O. R. Ogirigbo, and I. Inerhunwa. "Load-settlement characteristics of tropical red soils of southern Nigeria", *Eur. J. Eng. Res. Sci.*, vol. 4, no. 8, pp. 107-113, 2019.
- [13] Ikhile, C. "Geomorphology and hydrology of the Benin region, Edo state, Nigeria," *Int. J. Geosci.*, vol. 7, pp. 144-157, 2016.
- [14] Google maps. [Online]. Available <https://www.google.com/maps> [Accessed Dec. 13, 2020]
- [15] S. P. Howard, R. R. Donald, and G. Tchobanoglous, "Environmental engineering" McGraw-Hill International Editions, Civil Engineering Series, p. 45-78, 1985
- [16] EGASPIN, "Environmental Guidelines and Standards for the Petroleum Industry in Nigeria," Revised Edition, 2002, p. 23-26.
- [17] D. Raes, P. Willens, and F. Gbaguidi, "Rainbow - a software package for hydrometeorological frequency analysis and testing the homogeneity of historical data sets," In Proc. 4th Int. Workshop on Sustainable Management of Marginal Drylands, 27 – 30 January, Islamabad, Pakistan, 2006, pp. 41-55.
- [18] D. B. Levi, E. K. Julie, J. R. Olsen, R. S. Pulwarty, D. A. Raff, D. P. Turnipseed, et al. "Climate change and water resources management," A Federal Perspective, vol. 1331, pp. 1-72, 2009.
- [19] N. I. Ihimekpen, I. R. Ilaboya, L. O. Awah, "Non-parametric Mann-Kendall test statistics for rainfall trend analysis in some selected states within the coastal region of Nigeria," *J. Civ. Constr. Environ. Eng.*, vol. 3, no. 1, pp. 17-28, 2018.
- [20] Eviews 9.0, Tutorial Manual, p. 34-67.
- [21] O. C. Izinyon, L. I. Meindinyo, I. R. Ilaboya, "Evaluating the impact of seasonal variability on groundwater quality using multivariate analysis of variance," *Chem. Mater. Res.*, vol. 11, no. 10, pp. 41-54, 2019.
- [22] M. M. Gilbert, "Introduction to environmental engineering and science" Second edition, New Delhi: Prentice-Hall of India Private Limited, 2006, p. 413.
- [23] A. Caro, F. Legarda, L. Romero, M. Herranz, M. Barrera, F. Valiño, R. Idoeta, C. Olondo, "Map on predicted deposition of Cs-137 in Spanish soils from geostatistical analyses," *J. Environ. Radioact.*, vol. 115, pp. 53-59, 2013.
- [24] M. T. Karimi Nezhad, M. Ghahroudi Tali, M. Hashemi Mahmoudi, E. Pazira, "Assessment of As and Cd contamination in topsoils of Northern Ghorveh (Western Iran): role of parent material, land use and soil properties," *Environ Earth Sci*, vol. 64, pp. 1203-1213, 2011.